The International Journal of Advanced Manufacturing Technology (2018) 98:539–549
https://doi.org/10.1007/s00170-018-2250-0

ORIGINAL ARTICLE

Impact of pad conditioning on the bonnet polishing process

Bo Zhong [1,2] · Hongzhong Huang [1] · Xianhua Chen [2] · Jian Wang [2] · Ri Pan [3] · Zhongjiang Wen [2]

Received: 29 August 2017 / Accepted: 31 May 2018 / Published online: 13 June 2018
© Springer-Verlag London Ltd., part of Springer Nature 2018

Abstract
Pad conditioning is an important process for the improvement of tool removal characteristics by controlling tool surface conditions. This paper presents an experimental investigation, which attempts to reveal the influencing mechanism of pad conditioning on the tool removal characteristics in bonnet polishing process. By assistance of a dynamometer, a microscope, a laser displacement sensor, and a pressure distribution mapping system, multi-comparative group experiments are carried out to establish the correlation of pad conditions, polishing forces, and tool removal characteristic before and after pad conditioning. Through the experiments, three influencing mechanisms are identified: (1) the asperities of the tool surface become smaller and sharper after conditioning, which indicates that the real contact area between the polishing tool and the workpiece reduces, and the coefficient of friction (COF) increases as well, both leading to the improvement of tool removal efficiency; (2) the size of the asperity is determined by the granularity of the conditioner, for which the smaller the conditioner granularity is, the smaller the asperity will be, leading to the decrease of the real contact area; (3) the contour error of bonnet is improved after pad conditioning, so that the periodic amplitude of the polishing forces reduces and the symmetry of the tool influence function (TIF) becomes better. The influencing mechanism identified in this paper can be further served as critical foundation for the investigation on material removal determination through the optimization of pad conditioning process.

Keywords Pad conditioning · Bonnet polishing · Tool influence function · Coefficient of friction

1 Introduction

As a novel precision polishing technology, the bonnet polishing uses a flexible bonnet as a tool, which has the characteristics of good fit with curved workpieces and high removal efficiency. Bonnet polishing was first proposed by Walker [1], and completed the key technologies such as removal function model [2], process parameter optimization [3, 4], and processing path [5]. At present, this technology has been applied to the mass production of high-precision optical components required for major projects such as the European extremely large telescope (E-ELT) [6]. In addition, other research teams have also conducted research on the different difficult-to-machine objects such as the cobalt chrome alloys [7–9] and the tungsten carbide freeform molds [10] based on bonnet polishing. Since the bonnet tool interacts with the workpiece during the polishing process, the tool surface condition directly affects the material removal of workpiece, and therefore impacts the machining quality [11]. Consequently, how to achieve the controllability of the tool surface is an important issue for the optimization of the polishing process.

Pad conditioning is a commonly used method to control the tool surface condition during the polishing process. The pad conditioning not only improves the polishing effect, but also extends the pad lifetime and reduces the polishing cost. As a result, the conditioning process has been investigated by many researchers. Park et al. [12] indicated that the buffing process was able to control the pad surface conditions and ultimately exerted an effect on polishing characteristics including removal rate and break-in time in the chemical mechanical planarization (CMP) process. Li et al. [13] proposed that a

✉ Bo Zhong
zhongbo_foerc@163.com

[1] Department of Mechanical and Electrical Engineering, University of Electronic Science and Technology of China, Chengdu 610054, China

[2] Research Center of Laser Fusion, China Academy of Engineering Physics, Mianyang 621900, China

[3] College of Mechanical Engineering and Applied Electronics Technology, Beijing University of Technology, Beijing 100124, China

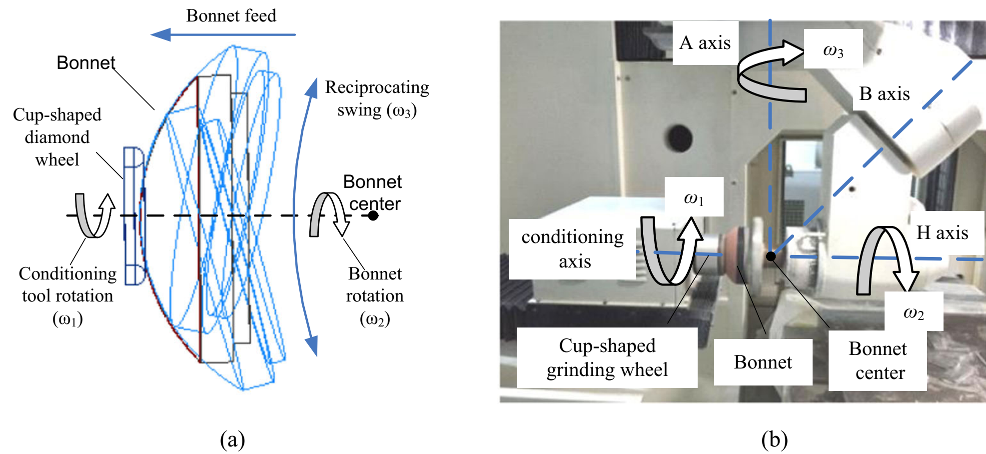

Fig. 1 In situ conditioning of bonnet based on the cup-shaped diamond wheel (**a**) principle (**b**) setup

diamond disc conditioner was employed to condition a polishing pad to restore the pad planarity and surface roughness in CMP. Zhou et al. [14] reported the influence of the diamond disc conditioning on the pad surface shape, and their experimental results showed that a concave pad surface shape can lead to a convex surface shape for the wafer. Yang et al. [15] investigated the effects of diamond size of CMP conditioner on wafer removal rates and defects for solid (non-porous) CMP pad with micro-holes and revealed that a smaller diamond conditioner generated the pad texture with finer and more regular pad asperities. Lee et al. [16] indicated that maintenance of the pad capacity played a key role in the machining of reliable elevations and investigated a conditioning effect on the machining capacity, deformation degree, and pad lifetime.

In summary, current studies revealed that the pad conditioning process can improve the tool surface characteristics and can also significantly enhance the stability of tool removal characteristics. However, current researches are mainly focused on the CMP process, and less have been laid on the sub-aperture polishing process (including bonnet polishing), especially the influencing mechanism of pad conditioning on the polishing tool removal characteristics. For this reason, multi-comparative group experiments are conducted to investigate the correlation among pad conditions, polishing forces, and tool removal characteristic before and after pad conditioning. Experimental results analysis and discussion on the impact of pad conditioning on the bonnet polishing process are presented based on the multi-comparative group experiments.

2 Experimental conditions and results

2.1 Experimental design and setup

Comparative experiments including stages of pad conditioning and optical polishing are designed and carried out in this section. Firstly, a bonnet tool covered with new polyurethane pad is used to polish the optical specimen. Subsequently, the pad is conditioned with rough particle and then polishes the specimen with identical parameters. Finally, the bonnet is conditioned again with fine particle and polishes the specimen with identical parameters. Within the above processes, the pad is conditioned (except for the first process) and measured before each polishing process to obtain the tool surface condition. The polishing forces are collected during each polishing process. The material removal of specimen is tested after each polishing process to evaluate the tool removal characteristic. Thus, by analyzing the results comprehensively, we

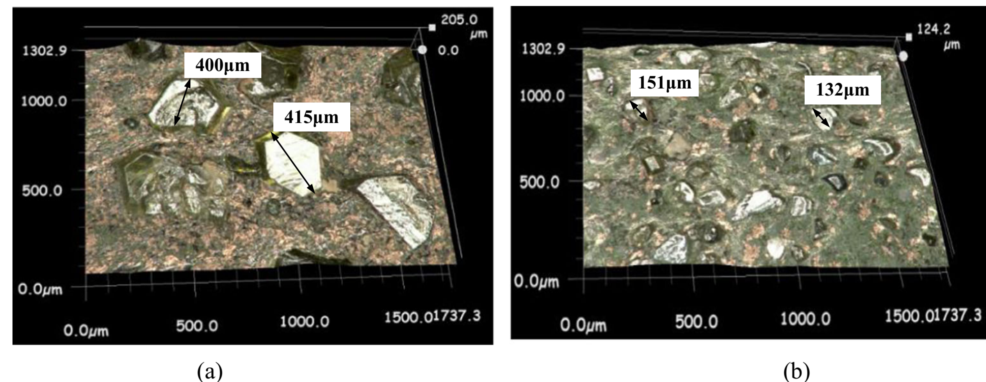

Fig. 2 Granularity of two conditioners. **a** Conditioner with rough particle. **b** Conditioner with fine particle

Table 1 The parameters of pad conditioning process

Conditioning type	Type of conditioner	Granularity of conditioner (μm)	Feed step (μm)	Conditioner rotational speed ω_1 (rpm)	Bonnet rotational speed ω_2 (rpm)	Reciprocating swing speed ω_3 (rpm)	Reciprocating swing angle (°)
Rough conditioning	No. 20	400	20	500	500	1.5	± 25
Fine conditioning	No. 80	150					

can investigate the impact of pad conditioning on the tool surface condition, and how it influences the polishing forces and the removal efficiency.

2.1.1 Pad conditioning process of bonnet tool

The principle and setup of in situ conditioning of the bonnet tool using a cup-shaped diamond is given in Fig. 1a, b respectively. The conditioning process includes the following steps: (1) the cup-shaped diamond wheel driven by the conditioning axis rotates with ω_1, (2) the bonnet driven by the H-axis rotates with ω_2, (3) the bonnet driven by the A-axis reciprocally swings with ω_3 around the bonnet center, (4) the bonnet driven by the x-axis of the machine tool moves to the conditioner, and (5) combined with the precise control of the bonnet and the conditioner, the pad covered on the bonnet is conditioned.

During the comparative experiments, the bonnet tool is conditioned two times with rough particle and fine particle, respectively. There are actually various granularities of the two cup-shaped diamond wheels (i.e., no. 20, no. 80). The profiles are measured by a digital microscope (VHX-5000, made by Keyence), which is presented in Fig. 2. As shown in Fig. 2a, the granularity of conditioner with rough particle is about 400 μm, and the granularity of conditioner with fine particle is about 150 μm as shown in Fig. 2b.

By referring to Figs. 1 and 2, the parameters of the two conditioning processes during the comparative experiments are listed in Table 1. After each conditioning process, the tool

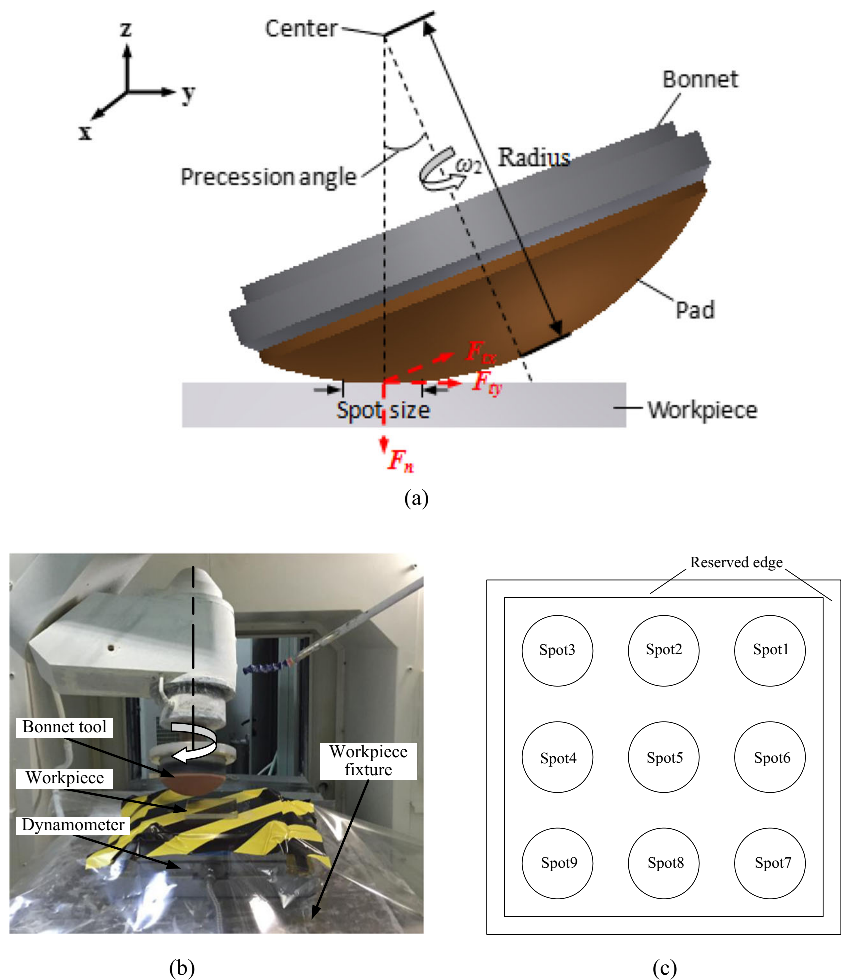

Fig. 3 Experimental specifications. **a** Schematic diagram of bonnet polishing. **b** Actual bonnet polishing and workpiece on the dynamometer. **c** Positions of spots

Table 2 Polishing experimental parameters after per conditioning

Bonnet radius (mm)	Spot size (mm)	Bonnet rotational speed ω_2 (rpm)	Bonnet pressure (MPa)	Precession angle (°)	Polishing time (s)
80	20	1000	0.15	23	4

surface condition is measured and used to polish the specimen. The specification of the polishing process is illustrated in the next section.

2.1.2 Specification of the polishing process

The specifications of the optical polishing process of the comparative experiments are illustrated in Fig. 3. As shown in Fig. 3, the removal process is conducted on a 100 mm × 100 mm × 10 mm SiO_2 glass, the peak-to-valley value (PV) of which is pre-polished to ~ 1 μm, and the reserved edges of both directions are 5 mm. Other experimental conditions are listed in Table 2. In addition, for each condition of bonnet tool (i.e., new, rough conditioning, fine conditioning), nine spots are polished to make sure the correctness of the results. Meanwhile, during the polishing process, the polishing forces on the workpiece containing the normal force (F_n) and the tangential force (i.e., the tangential force in x direction F_{tx}, the tangential force in y direction F_{ty}) are collected by a three-component dynamometer (model-9257B, made by Kistler), as described in our previous study [11]. After the polishing process, the spots are measured by a QED-made interferometer with model ASI(Q).

Based on the results from the conditioning process and the polishing process, the impact of pad conditioning on the tool surface condition, polishing forces, and the tool removal characteristic can be investigated.

2.2 Experimental results

2.2.1 Tool surface condition

Tool surface texture Surface texture of bonnet with three different states, which includes new pad, rough conditioning pad, and fine conditioning pad, is given in Fig. 4. These figures are measured by the three-dimensional microscopic system

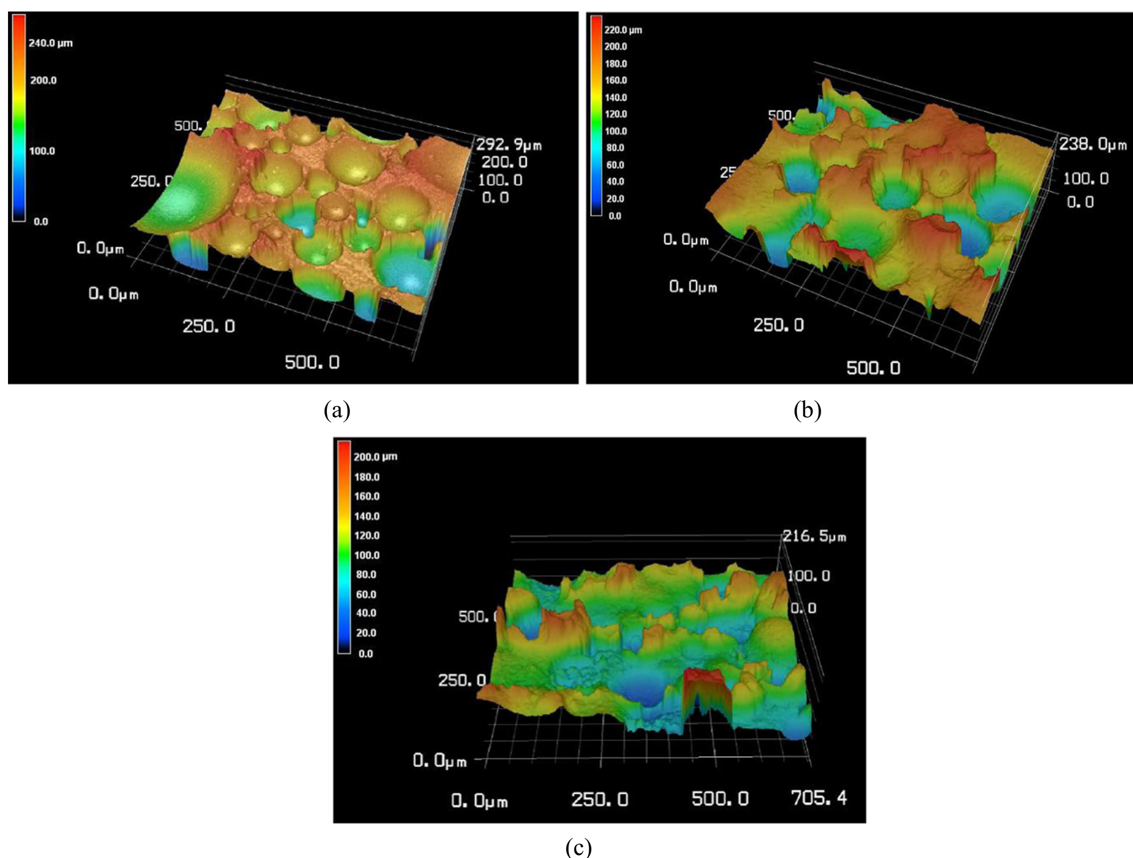

Fig. 4 Surface texture of bonnet with three different states measured by microscope. **a** New pad. **b** Rough conditioning pad. **c** Fine conditioning pad

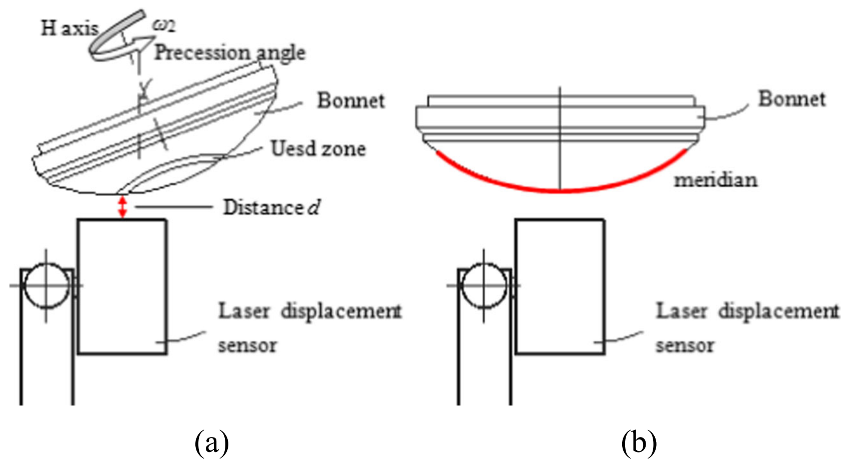

Fig. 5 Measuring schematic diagram of bonnet contour error by the laser displacement sensor. **a** Measuring diagram of zone error. **b** Measuring diagram of meridian error

(VHX-5000, made by Keyence). The amplitudes of the surface textures of the three pads with various conditions are about 292.9, 238, and 216.5 μm, respectively. Regarding to the details, the topography of the new pad shows that there are many irregular pores and asperities on the surface. After pad conditioning with rough particle, the asperities distribute irregularly. Subsequently, the microstructure of the pad after fine conditioning found remarkable differences from the new pad and rough conditioning pad. In detail, the asperities are smaller and sharper than those of new pad and rough conditioning pad. Consequently, through the conditioning process, a declining trend is identified for the amplitude of the tool surface texture, while the distribution of surface texture is irregular after conditioning. Moreover, the asperities on the tool surface become smaller and sharper, which is supposed to be dominated by the granularity of the conditioner, i.e., the smaller the granularity of the conditioner is, the smaller the size of the asperity will be.

Contour error of bonnet The contour error of bonnet includes the zone error and meridian error, of which the measuring principles are revealed in Fig. 5a, b, respectively. According to Fig. 5a, the used zone is the ring-shaped area on the bonnet, which contacts with the workpiece during the polishing process. The zone error defined in this study is the distance *d* along the vertical direction. When the bonnet has an oblique angle (precession angle), and rotates with angular velocity, the zone error is measured by the laser displacement sensor. The meridian represents the red line, shown in Fig. 5b, which crosses the vertex of bonnet. The meridian error is defined as the deviation of the meridian contour of bonnet and its closest spherical surface along the vertical direction, which is measured by the laser displacement sensor when the bonnet moves along to the spherical track driven by bonnet equipment.

The results of bonnet contour error are depicted in Fig. 6. It is found that the zone errors of bonnet with three different states (i.e., new, rough conditioning, fine conditioning) are about 450, 50, and 40 μm, respectively, implying that the initial zone error is very large. The zone error has an apparent reduction after the first conditioning process, while the zone error is further improved after the second conditioning process. On the other hand, the meridian errors of bonnet with three different states are closer, and mean values are all about 200 μm. As a result, it is evident that the zone error of bonnet has been improved significantly after conditioning, while the meridian error of bonnet changes slightly.

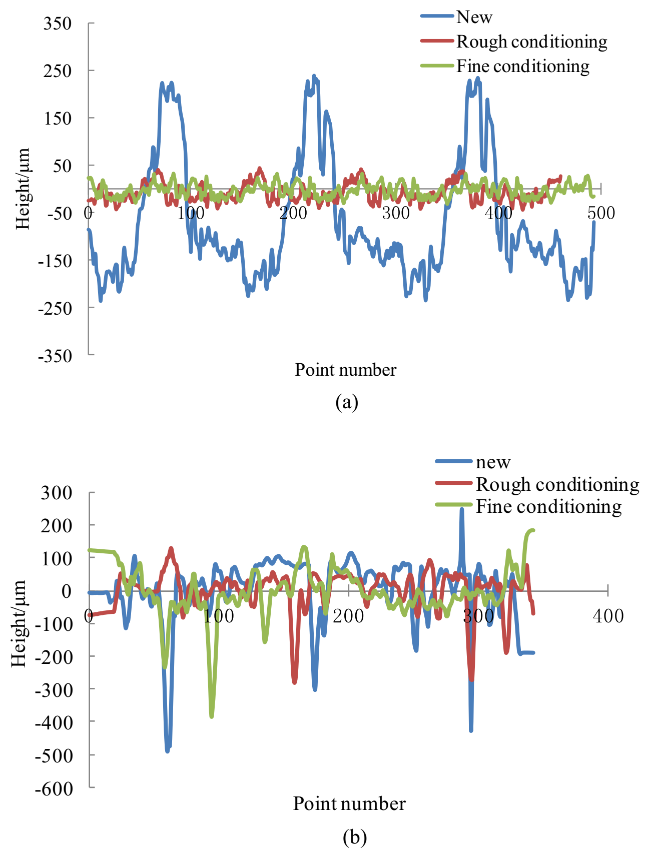

Fig. 6 Results of bonnet contour error. **a** Zone error. **b** Meridian error

2.2.2 Polishing forces

Figures 7 and 8 respectively reveal the polishing forces and the friction of coefficient, when the polishing tools with various surface conditions are used.

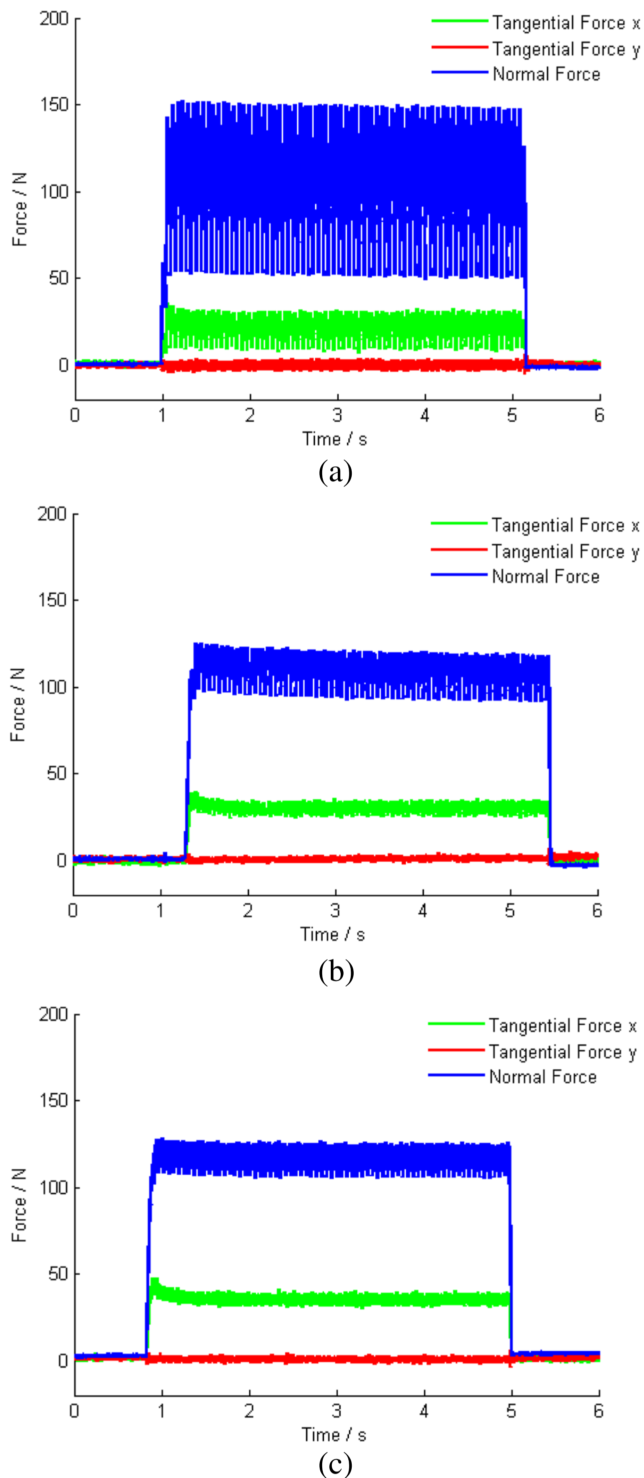

Fig. 7 The forces under three surface conditions. **a** New pad. **b** Rough conditioning pad. **c** Fine conditioning pad

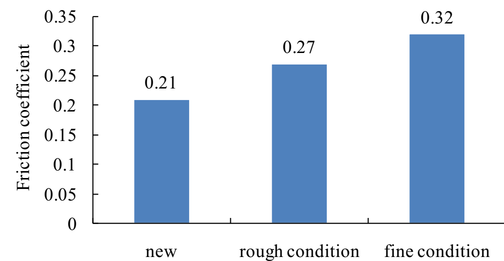

Fig. 8 The COF under three surface conditions

Since the x direction is consistent with the direction of rotation of bonnet (see Fig. 3a), the tangential force in the y direction is almost zero (see Fig. 7), and the tangential force in the x direction can be treated as the frictional force. Both the normal force and tangential force in the x direction are periodic, and the periodic amplitude of the normal force is larger than that of the frictional force. Moreover, the periodic amplitude of the normal force of the new pad is about 102.9 N, and the amplitudes reduce to 33.7 and 21.3 N, respectively, after rough conditioning and fine conditioning process. The periodic amplitudes of the frictional force with various surface conditions (i.e., new, rough conditioning, fine conditioning) are about 21.4, 8.9, and 6.7 N, respectively. Because the zone error is periodic when the bonnet rotates, the collected forces are periodic too. Furthermore, the zone error reduces after pad conditioning, resulting in the decrease of the periodic amplitude of forces.

Figure 8 reveals that there is a significant difference in the coefficient of friction (COF = tangential force/normal force) of three tool surface conditions. In detail, the COF of the new pad, rough conditioning pad, and fine conditioning pad is 0.21, 0.27, and 0.32 respectively. These differences imply that the conditioning process can change the COF, for which the smaller the granularity of the conditioner is, the larger the COF will be.

2.2.3 Removal characteristic

Spot shape Figure 9 shows the polished spots using tools with various surface conditions. Figure 10 reveals the contours of the spots in the X/Y direction. Figure 11 depicts the full width at half maximum (FWHM) of spots in the X/Y direction.

It can be identified from Fig. 9 that the spot of the new pad is obviously oval, and the spot shapes are significantly improved after conditioning, whose contours become approximately circular and symmetrical. As in Fig. 10a, in the case of the same spot size (16 mm) in X direction, the FWHM of spots in the X direction increases after conditioning process. In addition, the FWHM of spots in the X direction under three surface conditions (i.e., new, rough conditioning, fine conditioning) is 8.5, 10.5, and 11.5 mm, respectively (see Fig. 11a), which exhibits a significant rise by 23.5% after rough

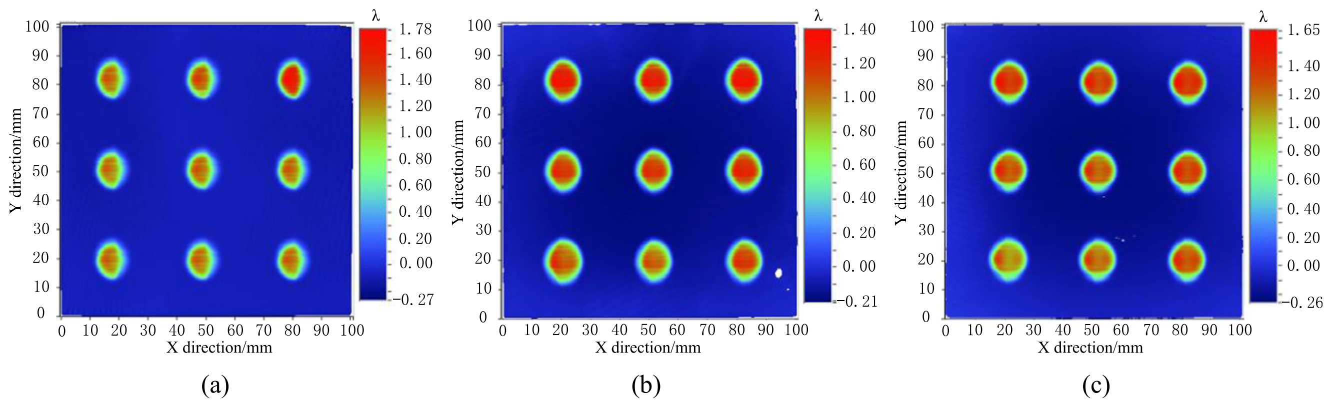

Fig. 9 Results of spots under three surface conditions. **a** New pad. **b** Rough conditioning pad. **c** Fine conditioning pad

conditioning, and a slight rise by about 9.5% after fine conditioning. In Fig. 10b, it can be figured out that in the case of the same spot size (20 mm) in the Y direction, the FWHM of spots in Y direction slightly increases after conditioning process. And the FWHM of spots in Y direction under three surface conditions (i.e., new, rough conditioning, fine conditioning) is 11.9, 13, and 13.2 mm, respectively (see Fig. 11b), which exhibits a slight rise about 10% after rough conditioning, and remains static after fine conditioning. The experimental results show that the shape of the polishing spot is improved, and the profile is symmetrical and approximately circular. In addition, the change of the FWHM of the polishing spot in the X direction is more obvious than that of spot in the Y direction.

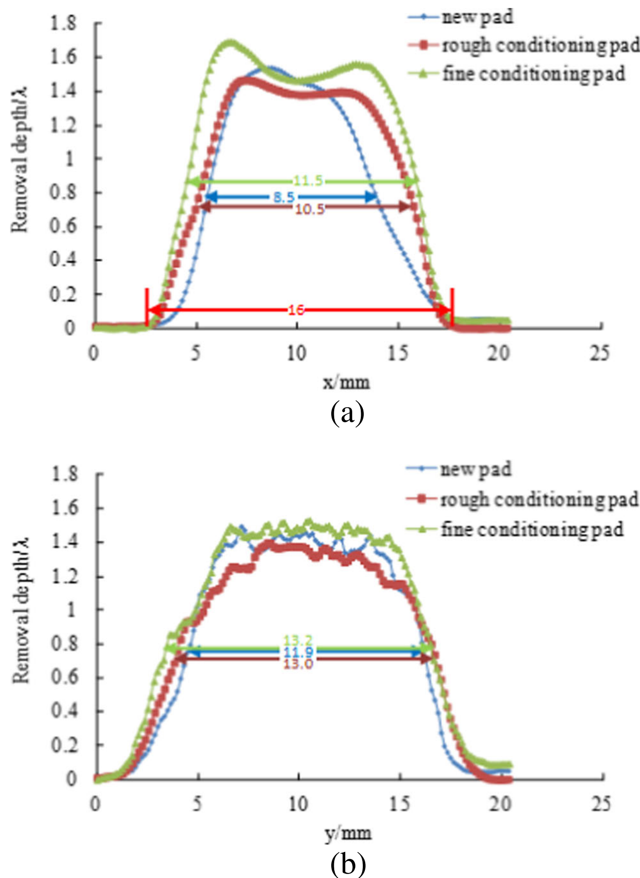

Fig. 10 The contour of spots under three surface conditions. **a** In the X direction. **b** In the Y direction

Removal efficiency It is found that the first few groups of spots have larger depth than the others. The reason is that the pad surface is harder and more rough at the first, which lead to the large tangential force for the initial spots (especially the first spot), and the tangential force falls down to keep consistent. Therefore, the statistical analysis of the removal efficiency is carried out by using the last six groups of spots. The results of removal efficiency are shown in Figs. 12 and 13.

According to Figs. 12 and 13, the removal depth of the new pad is about 1.6λ ($\lambda = 632.8$ nm), and the removal depth of the fine conditioning pad is 1.73λ, which exhibits a rise about 8.1%. In addition, the volume removal efficiency of the new pad is about 1.23 mm^3/min, and after rough and fine conditioning process, the efficiencies go up to 1.53 and 1.74 mm^3/min, which exhibit rises about 24.4 and 41.5% respectively. The experimental results indicate that the removal depth and volume removal efficiency are improved after the conditioning process, and the growth trend of the volume removal efficiency is more obvious than that of removal depth.

3 Discussion

Based on the above results, the impact of the pad conditioning process on the tool surface condition, the polishing forces, and the tool removal efficiency is discussed below.

3.1 Effect of pad conditioning on the tool surface condition, polishing forces, and tool removal efficiency

Current studies have demonstrated that the purpose of the conditioning process for polishing tool surface is to remove

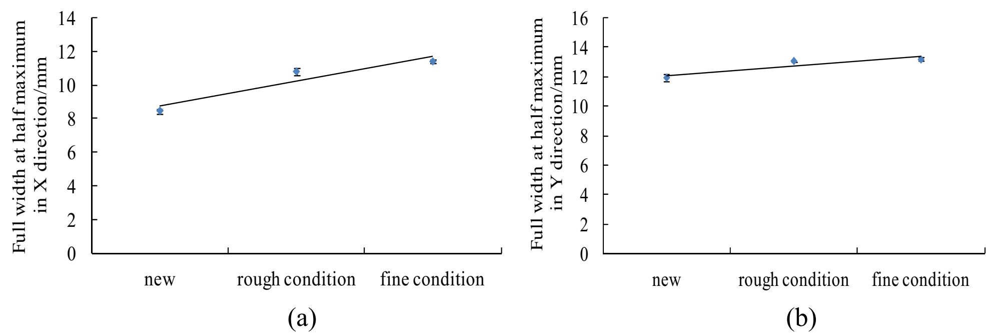

Fig. 11 Full width at half maximum of spots. **a** In the X direction. **b** In the Y direction

the worn areas so as to regenerate a new surface. Therefore, the wear and conditioning of the polishing tool are regarded as two reverse processes. Consequently, the influencing mechanism of pad conditioning on the tool surface condition, polishing forces, and tool removal efficiency can be analyzed from the opposite view of how tool wear affects the tool surface condition, polishing forces, and tool removal efficiency, based on the experimental results given in above sections.

3.1.1 The influencing mechanism of tool wear on the tool surface condition, polishing forces, and tool removal efficiency

Figure 14 reveals the three-dimensional and two-dimensional figures of the new and worn pad through the digital microscope. From Fig. 14, the pores and asperities of the new polishing pad are obviously visible and the edges are clear. Moreover, the asperity exhibits relatively flat and the surface has rough fine texture. On the contrary, the boundary between the pores and the asperities of the worn pad is blurred and the worn pad has the phenomenon of surface glazed. In addition, all asperities become smooth, and the height between pore and asperity is slightly lower than that of the new pad.

According to the previous studies [17], the real contact area between the polishing tool and the workpiece is an important variable for explaining the influence mechanism of tool wear. It is the sum of the asperities that actually touches the workpiece on the nominal contact area. These asperities bear all the polishing forces directly and support the particles to remove the workpiece material. Based on the above results, the influencing mechanism of tool wear are summarized and shown in Fig. 15a. The asperity of the new pad is approximately trapezoidal, whose contact area with the workpiece is the projective black circle. Subsequently, due to the worn of polishing pad, the asperities become the arc-shaped, whose contact area with the workpiece is the projective red circle. The difference between the area of the two circles (i.e., the black circle, the red circle) is the increase in the real contact area caused by the worn of the polishing pad. On this condition, in the case of the same polishing force, since the real contact area increases, the real polishing pressure decreases. According to the Preston law, the removal efficiency declines with the wear of pad.

3.1.2 The influencing mechanism of pad conditioning on the tool surface condition, polishing forces, and tool removal efficiency

As the reverse process of the wear process, the principle of the influencing mechanism of pad conditioning can be expressed as Fig. 15b. The asperity of the new pad is initially trapezoidal, whose contact area with the workpiece is the projective black circle. Subsequently, through the conditioning process, the large asperity is cut into several small asperities with trapezoidal shape, whose contact areas with the workpiece are the projective blue circles. The most obvious difference between the worn and conditioning processes of polishing tool mainly lies in two typical aspects. The asperity of the polishing pad becomes smooth, and the real contact with the workpiece increases in the wear process. While the asperity becomes

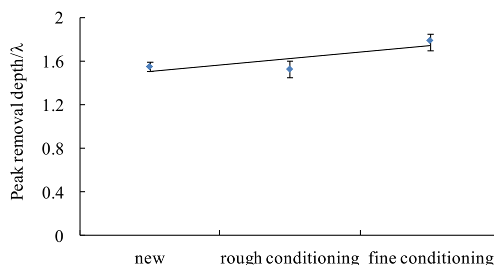

Fig. 12 The effect of conditioning on the removal depth

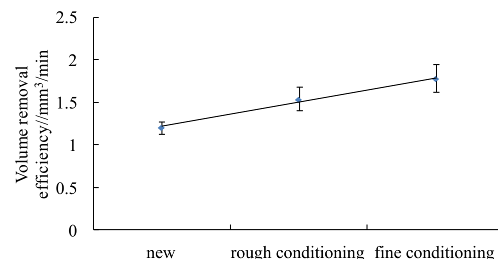

Fig. 13 The effect of conditioning on the volume removal efficiency

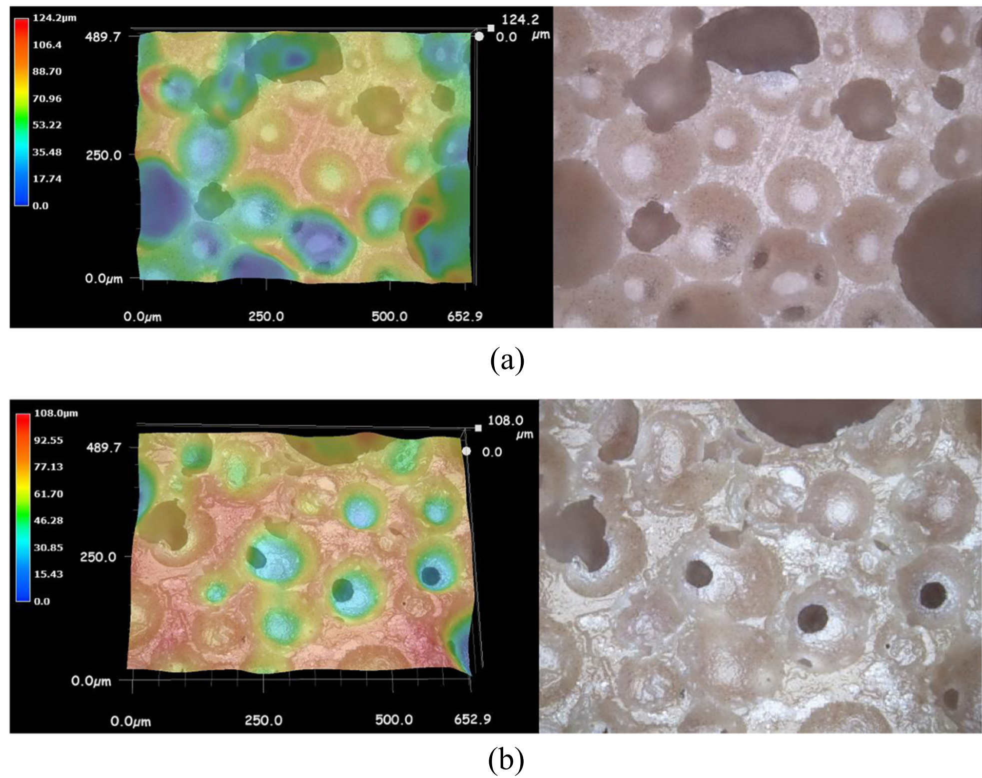

Fig. 14. 3-D images and SEM images (× 500) taken with new pad (**a**) and worn pad (**b**)

small and sharp, the real contact with the workpiece decreases in the conditioning process.

The above argument of the variation of the asperities shape after conditioning can also be supported by the results presented in Fig. 16. The distribution of the asperities of the new pad is regular and the size range is 0~150 μm. However, the large asperity of the pad is about 120 μm after the rough conditioning process, and the large asperity of the pad distribution is about 60 μm after fine conditioning process.

According to the above analysis, it can be argued that the main reason for the rise of the frictional force and COF after conditioning is that the asperity becomes smaller and sharper, resulting in smaller real contact area. We deduced that the surface of the polishing tool after conditioning becomes rough, which may enhance the constraining force of the polishing tool surface to the abrasive particles, thus making the removal of some abrasive particles from rolling friction to sliding friction. Another factor that might induce the higher frictional force and COF is more polished abrasive particles in the contact area during polishing.

To verify the above argument of real contact area in different pad conditions, the contact areas within the three pads (i.e., new pad, rough conditioning pad, fine conditioning pad) and an optical glass are examined by the pressure distribution mapping system (FPD-8010E, made by FIJIFILM Corporation). Figure 17 shows results of real contact area measurements of the three pads. The blue areas on these images indicate that the pad surface is not in contact with the

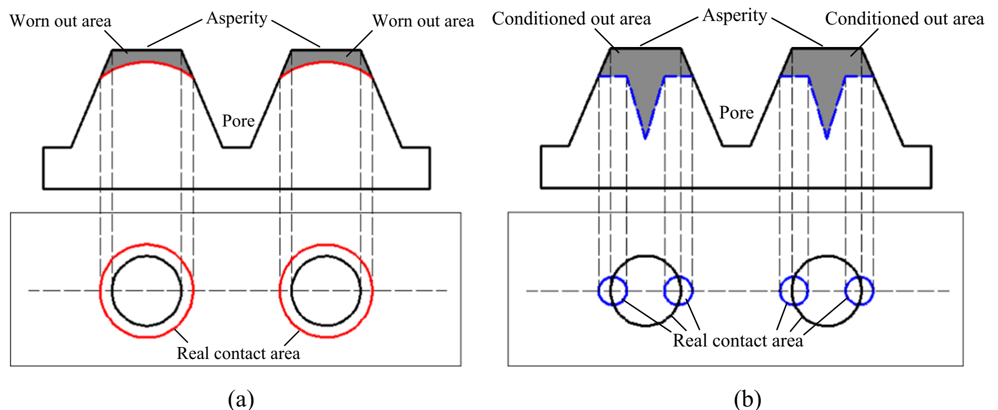

Fig. 15 Real contact area in the different pad conditions. **a** New pad to worn pad. **b** New pad to conditioned pad

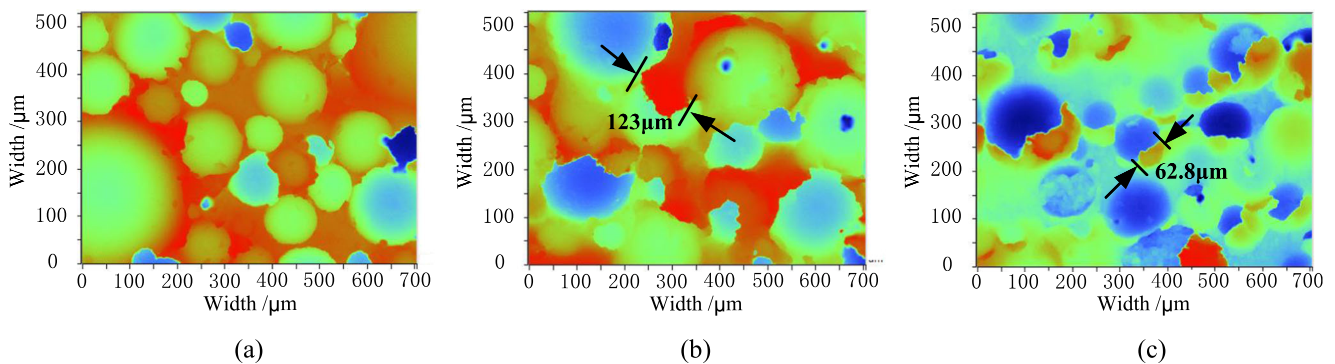

Fig. 16 Contour plots in the different pad conditions. **a** New. **b** Rough conditioning. **c** Fine conditioning

glass, and the other colored areas indicate that the pad is in contact with the glass. The real contact area ratios of three pads (i.e., new pad, rough conditioning pad, fine conditioning pad) are about 15.2, 9.2, and 6.9%, respectively. Therefore, after rough and fine conditioning processes, the real contact area ratios are decreased by about 39.5 and 54.2% respectively. From this result, the argument that the real contact area between the wafer and the fine conditioning pad will be smaller than the rough conditioning pad is validated.

In the case of maintaining the normal force (shown in Fig. 7) and the nominal contact area (i.e., the spot size, shown in Fig. 10), the real contact area decreases after pad conditioning, resulting in increasing the frictional force and the COF (shown in Fig. 8). According to the Preston law, it can be argued that the rise of the frictional force and COF leads to the improvement of the removal efficiency. Furthermore, the effect of the conditioning process with different conditioners on the removal efficiency is similar to the results in the CMP process reported by Yang [15], which can further justify the argument derived above.

3.2 Effect of conditioning process on the shape of TIF

As stated above, another important factor of surface condition of the bonnet is the contour error, including the zone error and meridian error. According to the results in section 2.2, the zone error of the bonnet is greatly improved after pad conditioning, while the periodic amplitude of the polishing force reduced and the symmetry of the TIF becomes better. Thus, it is inferred that the stability of the polishing force and the symmetry of the TIF are sensitive to the zone error and meridian error. Therefore, in order to ensure the consistency of the size of the TIF, the static pressure sensor is used to ensure that the size of the bonnet contact with the workpiece is consistent, as described in our previous study [11]. When the zone error is small, more areas of bonnet contact with the workpiece, therefore the FWHM of TIF is larger. In the experiment, the FWHM of TIF in the X\Y direction increases after the rough conditioning process, and the increase of the FWHM in the X direction is more obvious than that of FWHM in the Y direction.

It is concluded that the zone error and meridian error affect the shape of TIF in the X direction and Y direction respectively. The variety of the shape of TIF in the X direction is remarkable due to the improvement of zone error. Since the initial meridian error of the bonnet in the experiment is better, and the meridian error slightly changes after conditioning, the variety of the shape of TIF in the Y direction is slight. It can be identified that the bonnet contour error has an influence on the shape of the TIF. Therefore, the pad conditioning process and the corresponding measuring method can effectively guarantee the quality of the bonnet contour, which can ensure the stability of the TIF and the controllability of the bonnet polishing process.

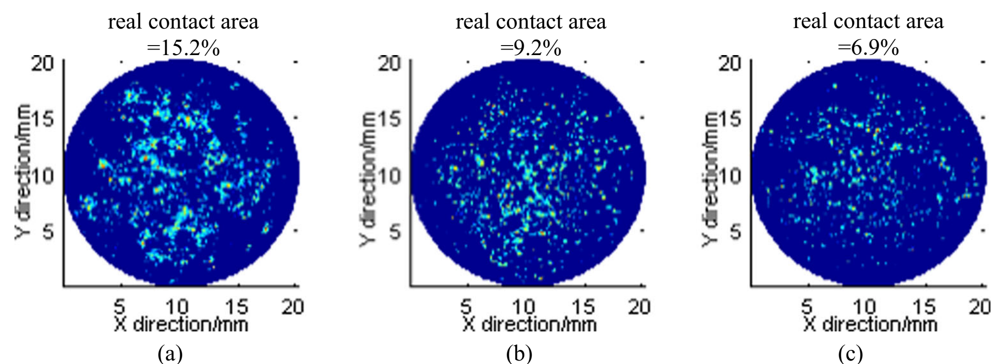

Fig. 17 Results of real contact area measurements of the three pads. **a** New pad. **b** Pads conditioned by 400 mm. **c** 150-mm diamonds

4 Conclusion

Aiming to investigate the influencing mechanism of pad conditioning on the tool condition, the polishing force, and the removal characteristics, the multi-comparative group experiments are conducted to reveal the correlation of pad conditions, polishing forces, and tool removal characteristics. The following conclusions are obtained:

(1) Through pad conditioning, the asperities of tool surface are smaller and sharper, leading to the growth of the COF and frictional force between the tool and the workpiece. Moreover, the real contact area between the tool and the workpiece decreases due to the variation of the asperities shape, which leads to the rise of the pressure on the polished area. For the above reasons, the tool removal efficiency is enhanced after conditioning. Compared with the new pad, the volume removal efficiencies with the rough and fine conditioning pads are increased by about 24.4 and 41.5% respectively. In addition, the size of the asperity of pad and the real contact area are related to the granularity of the conditioner. The smaller the granularity of the conditioner is, the smaller the asperity and the real contact area will be.

(2) The effect of conditioning process on the asperity and the real contact area is opposite to the effect of wear process. In detail, it is observed that the asperity of the polishing pad becomes smooth, and the real contact with the workpiece increases in the wear process. Although, the asperity becomes small and sharp, the real contact with the workpiece decreases in the conditioning process. After rough and fine conditioning processes, the real contact area ratios are decreased by about 39.5 and 54.2% respectively.

(3) The pad conditioning is found to have a great impact on the stability of the polishing forces and the symmetry of the TIF. Indeed, along with the improvement of the contour error of the bonnet after pad conditioning, the periodic amplitude of the polishing forces reduces and the symmetry of the TIF becomes better.

Acknowledgements We appreciate the invaluable expert comments and advices on the manuscript from all anonymous reviewers.

Funding information This work was financially supported by the Science Challenge Project (No. JCKY2016212A506-0502), the National Nature Science Foundation of China (No. 51705011), and the Youth Talent Fund of Laser Fusion Research Center, CAEP. (No. RCFCZ1-2017-6).

Publisher's Note Springer Nature remains neutral with regard to jurisdictional claims in published maps and institutional affiliations.

References

1. Bingham RG, Walker DD, Kim DH, Brooks D, Freeman R, Riley D (2000) A novel automated process for aspheric surfaces. Proc SPIE, the International Symposium on Optical Sci Technol, 4093: 445–448
2. Li HY, Walker DD, Yu GY, Sayle A, Messelink W, Evans R, Beaucamp A (2014) Edge control in CNC polishing, paper 2: simulation and validation of tool influence functions on edges. Opt Express 21(1):370–381
3. Walker DD, Brooks D, King A, Freeman R, Morton R, McCavana G, Kim S (2003) The 'precessions' tooling for polishing and figuring flat, spherical and aspheric surfaces. Opt Express 11(8):958–964
4. Walker DD, Beaucamp ATH, Bingham RG, Brooks D, Freeman R, King SW, King A, McCavana G, Morton R, Riley D, Simms J (2003) Precessions aspheric polishing: new results from the development programme. Proc SPIE, Optical Manufacturing and Testing V (5180):15–28
5. Dunn CR, Walker DD (2008) Pseudo-random tool paths for CNC sub-aperture polishing and other applications. Opt Express 16(23): 18942–18949
6. Yu GY, Walker DD, Li HY (2012) Research on fabrication of mirror segments for E-ELT. Proc SPIE, 6th International Symposium on Advanced Optical Manufacturing and Testing Technologies 8416:841602
7. Zeng S, Blunt L (2014) An experimental study on the correlation of polishing force and material removal for bonnet polishing of cobalt chrome alloy. Int J Adv Manuf Technol 73(1–4):185–193
8. Zeng S, Blunt L (2014) Experimental investigation and analytical modelling of the effects of process parameters on material removal rate for bonnet polishing of cobalt chrome alloy. Precis Eng 38: 348–355
9. Zeng S, Blunt L, Racasan R (2014) An investigation of the viability of bonnet polishing as a possible method to manufacture hip prostheses with multi-radius femoral heads. Int J Adv Manuf Technol 70(1–4):583–590
10. Beaucamp A, Namba Y, Inasaki I, Combrinck H, Freeman R (2011) Finishing of optical moulds to λ/20 by automated corrective polishing. CIRP Ann Manuf Technol 60:375–378
11. Zhong B, Chen XH, Pan R, Wang J, Huang HZ, Deng WH, Wang ZZ, Xie RQ, Liao DF (2017) The effect of tool wear on the removal characteristics in high-efficiency bonnet polishing. Int J Adv Manuf Technol 91:3653–3662
12. Park K, Park J, Park B, Jeong H (2008) Correlation between break-in characteristics and pad surface conditions in silicon wafer polishing. J Mater Process Technol 205:360–365
13. Li ZC, Baisie EA, Zhang XH (2012) Diamond disc pad conditioning in chemical mechanical planarization (CMP): a surface element method to predict pad surface shape. Precis Eng 36(2):356–363
14. Zhou YY, Davis EC (1999) Variation of polish pad shape during pad dressing. Mater Sci Eng B68:91–98
15. Yang JC, Choi JH, Hwang T, Lee C, Kim T (2010) Effects of diamond size of CMP conditioner on wafer removal rates and defects for solid (non-porous) CMP pad with micro-holes. Int J Mach Tool Manu 50(10):860–868
16. Lee ES, Cha JW, Kim SH (2013) Evaluation of the wafer polishing pad capacity and lifetime in the machining of reliable elevations. Int J Mach Tool Manu 66:82–94
17. JEONG H, LEE H, CHOI S, LEE Y, JEONG H (2012) Prediction of real contact area from microtopography on CMP pad. J Adv Mech Des Syst 6(1):113–120